FULL PAPER

Mesoporous Protein Particles Through Colloidal $CaCO_3$ Templates

*Stephan Schmidt, Muriel Behra, Katja Uhlig, Narayanan Madaboosi, Laura Hartmann, Claus Duschl, and Dmitry Volodkin**

Porous colloidal particles can be tailored using templating techniques to maximize their effectiveness for a wide range of applications, including separation, catalysis, and drug delivery. However, templating usually involves harsh and complex preparation conditions, thereby complicating the fabrication of sensitive bio-functionalized particles. Here a simple, yet versatile and mild approach us used to create porous protein particles using mesoporous $CaCO_3$ colloids as sacrificial templates. The three-step preparation procedure involves infiltrating the colloidal templates with the protein by solvent evaporation, protein crosslinking, and removal of $CaCO_3$. Using this method one can obtain porous particles consisting of virtually any protein. To explore the applicability of the particles for various scenarios particles composed of different proteins are fabricated focusing on hemoglobin and trypsin and particle morphology, porosity, mechanical properties, the protein redox state, and enzymatic activity are determined. The results show that the nanoporous template structure is replicated and that the proteins are fully functional. By varying preparation conditions such as crosslinker concentration and protein content the elastic modulus is adjusted in the range of red blood cells. This ensures high deformability upon flow in microchannels and makes the porous protein particles a versatile platform for biomedical applications.

1. Introduction

One of the major challenges the pharmaceutical industry is facing today is the formulation of new protein therapeutics in order to optimize their stability, activity, and efficiency for specific administration routes.[1] An important strategy is the formulation of protein drugs into crosslinked aggregates such as microparticles[2] and crystals[3] or encapsulation by various techniques including drying and embedding into polymer matrices.[4,5] Such systems offer many advantages for example increased circulation time in the blood, protection against degradation or site specific delivery.

Another important application of protein particles is their use for biotechnological processes such as biocatalysis.[6] The particle systems for these applications can be very simplistic. Often they are merely composed of crosslinked enzyme aggregates (CLEAs) without an additional carrier. Such CLEAs possess many advantages over enzyme solutions and enzymes bound to carriers: cost efficiency due to possible recovery by filtration, highly concentrated enzyme activity in the aggregate as well as high stability.[7] In general they are prepared by precipitation of the protein using salts or organic solvents and subsequent covalent crosslinking by glutaraldehyde (GA) and other agents.[8] Importantly, due to their porosity and the resulting high internal surface area the activity of CLEAs particles is comparable to the freely dissolved enzyme molecules.[9,10] Also combinations of enzymes such as glucose oxidase and catalase to improve activity retention of the oxidase have been documented.[11] In principle such simple but highly active protein particles would also be interesting for biomedical applications. However the polydispersity of these systems prohibits clinical applications where precise control over size, porosity, surface chemistry, composition, and mechanical properties are mandatory. For example material parameters such as size, surface chemistry, and deformability greatly affect the circulation time of microparticles in the vascular system.[12] Moreover, size and accessible surface area (porosity) are imperative characteristics to ensure predictable catalytic or therapeutic efficiency of the protein particles.[6,7,9]

Although porous particles composed from crosslinked proteins/enzymes have good potential in drug delivery, biotechnology and biocatalysis, the preparation challenges still impede the wide use of such systems. Typically, porous materials are prepared from emulsions,[13] by solvent evaporation,[14] or precipitation.[15,16] Templating techniques[17,18] are used when precise control over material properties, like composition, morphology and porosity, is desired. In principle these parameters can be controlled by selection of the template. However, templating techniques often involve harsh preparation conditions, for example pyrolysis or hydrofluoric acid etching to remove polymer[18] or silica templates.[19] This, as well as other

Dr. S. Schmidt, M. Behra, L. Hartmann
Max Planck Institut für Kolloid- und Grenzflächenforschung, Am Mühlenberg 13, Potsdam-Golm, 14476, Germany
Dr. K. Uhlig, N. Madaboosi, Dr. C. Duschl, Dr. D. Volodkin
Fraunhofer IBMT, Am Mühlenberg 13, Potsdam-Golm, 14476, Germany
E-mail: Dmitry.Volodkin@ibmt.fraunhofer.de

DOI: 10.1002/adfm.201201321

techniques e.g. involving organic solvents could damage the protein structure by irreversible denaturation, deswelling and collapse of the porous scaffold. To obtain functional porous protein particles it is therefore imperative to choose templates that can be dissolved at mild conditions in aqueous media. Porous $CaCO_3$ microparticles fulfill this requirement and have been successfully used as hard templates for the synthesis of pure pharmaceutical protein particles[2,20] and polyelectrolyte capsules containing proteins.[5,21,22] However theses studies were not aimed to introduce and to utilize mesoporous morphologies in the particles. Here, we now want to use $CaCO_3$-based templates but instead synthesize mesoporous protein particles.

Therefore, in the present work we exercise $CaCO_3$ templating such, that the mesoporous structure of the $CaCO_3$ microparticles[16] is replicated as inverse structure. Using this approach we aim at crosslinked protein assemblies with well defined size, internal structure, activity and mechanical properties. To achieve this goal, a straightforward preparation procedure involving template infiltration by solvent evaporation, protein crosslinking using GA and removal of the templates by EDTA is developed. We then use optical microscopy, AFM, and SEM to analyze internal structure of various porous protein particles and investigate the applicability of hemoglobin particles as a red blood cell mimic[23–25] and trypsin particles as a CLEA.[26] The novel template based preparation procedure ensures a high internal surface area and deformability of the particles. Consequently, we investigate the enzymatic activity of the trypsin particles and conduct micromechanical studies on hemoglobin particles with varied crosslinker ratio to mimic the mechanical properties of red blood cells. This approach may enhance the particles' vascular circulation time and compatibility to filtration barriers in living organisms.

2. Results and Discussion

2.1. Particle Preparation

The preparation of the porous protein particles relied on a straightforward procedure based on $CaCO_3$ template particles (**Scheme 1**). In a preceding step templates with well defined size and porosity were prepared.[22] The $CaCO_3$ templates can be formed at supersaturation by mixing $CaCl_2$ and Na_2CO_3 under vigorous stirring and initiated by heterogeneous precipitation.[27] The resulting $CaCO_3$ templates are constituted of non-randomly arranged vaterite crystallites that tend to radiate from the centre forming pores arranged like wheat-sheaves.[16] This type of structure facilitates the infiltration of protein into the templates which is conducted by evaporation of water from the protein solution in the presence of the template particles (Scheme 1A). Due to evaporation and capillary action the protein solution recedes into the pores, effectively transporting the protein into the templates.[28] Under controlled agitation during evaporation and keeping the protein/$CaCO_3$ weight ratio below 10%, the protein can be transferred completely and selectively into the pores. In a previous work we used the same principle to prepare porous polyethylene glycol particles and showed the selectivity of the loading process in dependence of preparation condition such as the loading ratio and template type.[29] Then, the filled template particles are re-dispersed in high ionic strength solutions of kosmotropic salts (e.g., 4 M Na_2SO_4) to suppress dissolution of the protein from the templates. Vigorous agitation by high shear stirring and also moderate ultrasonication facilitates dispersion and removes excess of protein from the template surface. Next, the protein is crosslinked by addition of GA (Scheme 1B). After several washing steps pure protein particles can be obtained by dissolution of the template in EDTA (Scheme 1C and Supporting Information S2).

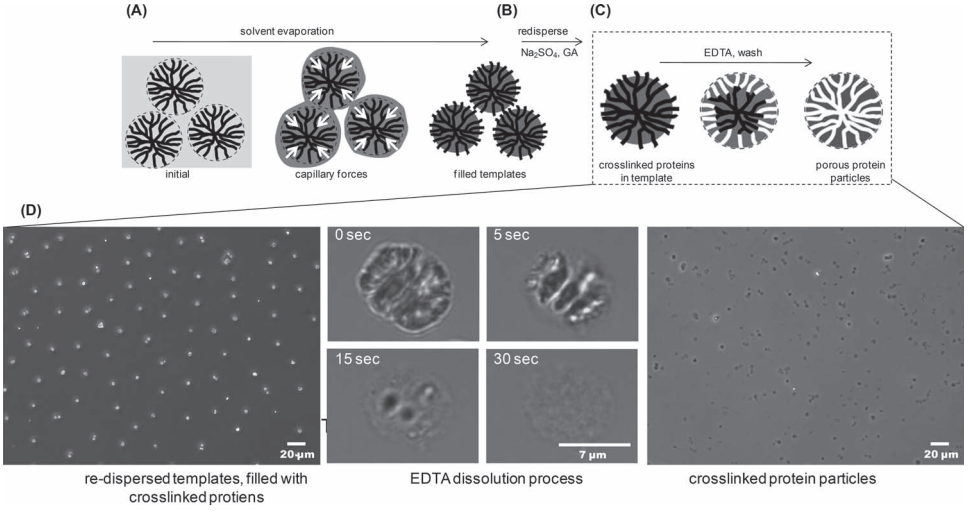

Scheme 1. Preparation of porous protein particles: A) infiltration of the templates by solvent evaporation, B) crosslinking of the protein in the templates, and C) removal of the $CaCO_3$ templates to obtain the porous protein particles. D) Optical microscopy shows that individual well defined particles can be obtained by the calcium carbonate templating approach. The middle panel shows the dissolution of a $CaCO_3$ template (63× objective, brightfield illumination, 6.5 µm templates). The left and right panels present particles before and after template dissolution (20× objective, phase contrast optics, 6.5 µm templates).

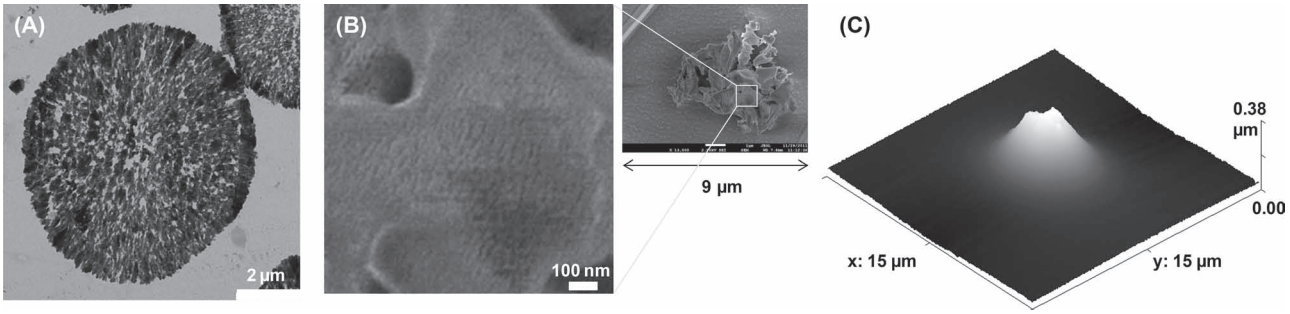

Figure 1. A) TEM image of $CaCO_3$ template 6.5 µm. B) Cryo-SEM image of a porous hemoglobin particle. C) AFM image of a dried hemoglobin particle with a volume of 3 μm^3.

2.2. Particle Morphology

The template dissolution process was observed via optical microscopy during the preparation (Scheme 1D). The presented particles were prepared according to the standard procedure using 6.5 µm $CaCO_3$ templates (Supporting Information S4) with a crosslinker/protein ratio of 0.03 w/w. Single particles resembling the spherical shape of the templates were obtained by this straightforward procedure. The average size of the presented hemoglobin particles was 5.8 ± 0.95 µm. Similar sizes were observed for particles composed of other proteins (Supporting Information S2 and S3). The particles show a narrow size distribution when compared to classic precipitation methods that typically result in larger particles and size distributions.[9,10,30] Furthermore, methods relying on protein precipitation or adsorption on templates need to be adapted when varying the protein because precipitation aggregate formation depends on the solubility, isoelectric point and molecular weight. This is not the case for particle formation through $CaCO_3$ templating: Capillary forces are the main factor for loading and particle formation as they draw the protein solution into the templates and are independent of the kind of protein used. As a result, particles composed of different proteins such as trypsin, insulin and lysozyme always resembled the shape and size of the template without adapting the preparation procedure (Supporting Information S3).

Well defined particle sizes but also well controlled internal structures are highly desired. The porous structure of the $CaCO_3$ templates are constituted of crystallites (vaterite mainly) of about 30–100 nm in size (**Figure 1** and Supporting Information S4). The void space between these fibers presents a channel-like structure with interconnected pores of about 30 nm in size as measured by nitrogen adsorption and seen via TEM.[22] Exact inverse replicates would present channel-like structures with interconnected pores of 30–100 nm held together by a crosslinked protein network with an average thickness of 30 nm for the protein assembly. To test this assumption we investigated the porosity of hemoglobin particles.

To visualize the overall structures we imaged hemoglobin particles via cryo-scanning electron microscopy (cryo-SEM, Figure 1B). The results indicate a loose structure of low protein content, however, the resulting morphologies did not resemble an inverse replicate of the template particles. Instead, the particle appears collapsed with very few pores that have larger diameters than the expected 30–100 nm. Apparently freeze-etching during sample preparation caused drying of the particles and collapse of the pores. This is probably due to the large number of voids and low protein content (high water content) resulting in a low structural integrity in dry state. AFM imaging of protein particles dried on a solid substrate under ambient conditions revealed an average volume of 3 ± 0.6 μm^3 of the dried and completely collapsed particle (Figure 1C). When compared to the average volume of the swollen particles in water of 113 μm^3, the water content by volume of the particles is 97%. This high water content indicates the presence of water filled pores in the protein particles, e.g., by comparison with the lower water content of highly swollen polymers gels.[29]

Thus, due to the low stability of the protein particles upon drying we could not image their porous structures directly. Therefore we conducted permeability studies by confocal microscopy with fluorescently labeled high molecular weight dextrans (**Figure 2**). The fluorescence intensity profiles (Figure 2, insets) show the amount of the dextrans inside or outside of

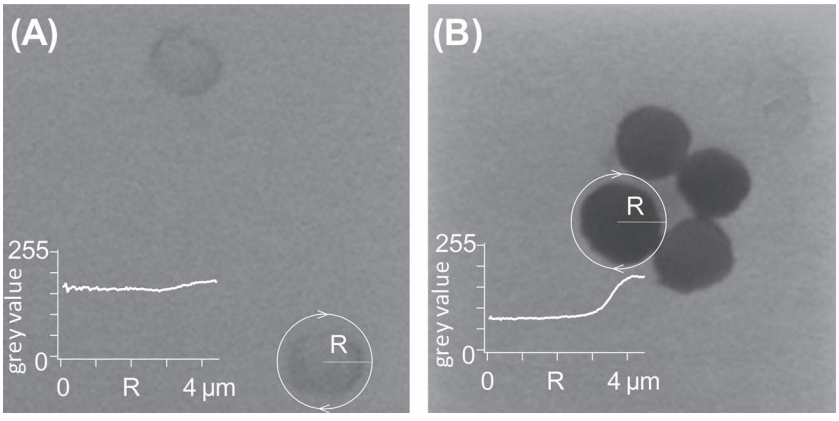

Figure 2. Permeability study with fluorescently labeled dextrans on porous hemoglobin particles A) 500 kDa FITC dextran, which diffuses freely into the particles, and B) 2000 kDa FITC dextran, which only partially enters the particle.

the hemoglobin particles after one hour of incubation (in terms of contrast or grey value). The experiments revealed that dextrans with a molecular weight below 500 kDa diffused freely into the particles (90% fluorescence inside compared to outside), whereas 2000 kDa entered the particles to a lesser extent (42% fluorescence inside). The hydrodynamic diameter of the two dextrans was 29 nm (500 kDa) and, respectively, 54 nm (2000 kDa).[31] Therefore we can assume the majority of pore diameters are distributed between 29 and 54 nm. An additional permeability study with fluorescent nanoparticles with a diameter of 103 nm showed that almost none of the fluorescent nanoparticles diffused into porous protein particle (Supporting Information S6). This indicates that the protein particles are indeed mesoporous with a pore size below 100 nm. Overall the permeability study reflects the expected range of the pores due to the vaterite crystallite sizes of the template particles (30–100 nm, Figure 1A, Supporting Information S4). This shows that we obtained structures that are most likely true inverse replicates from the mesoporous internal structure of $CaCO_3$ templates as has been also shown for porous polyethyleneglycol particles prepared through $CaCO_3$ templating.[29] On the other hand, the expected maximum pore size should correspond to the size of the largest crystallites in the templates of around 100 nm (see Supporting Information S4). However the permeability study is not sensitive toward these larger cavities in the porous network as the fluorescent marker cannot permeate trough the majority of channels that are between 29 and 54 nm in diameter.

2.3. Activity of the Protein Particles

So far we have shown that the method allows for the preparation of structural replicates of the $CaCO_3$ templates with proteins. In the next step we studied the activity of trypsin and hemoglobin after transformation into porous particles. First we studied the enzymatic activity of trypsin particles for different degrees of crosslinking and varied particles sizes. Crosslinking was conducted for different GA concentrations of 0.25 mM and 25 mM corresponding to a GA/protein weight ratio of respectively, 0.003 and 0.3. The enzymatic activity was determined photometrically[32] and compared to a non-crosslinked trypsin in solution. The slopes of the curves shown in **Figure 3** correspond to the conversion rate of the BAEE substrate and thus the catalytic activity of the trypsin formulations. For particles prepared from 6.5 µm sized templates with a GA/protein ratio 0.03, we observed activities of about 25% compared to the trypsin standard. When increasing the GA/protein ratio to 0.3 a further reduced activity to 13% was observed. This reduction in activity is expected[11] and can be directly attributed to the crosslinking agent GA altering the active sites of the enzyme. Larger particles prepared from 15 µm sized templates with a protein/crosslinker ratio 0.03 showed a higher activity of 33% as compared to particles prepared from 6.5 µm templates. This is somewhat unexpected because larger particles typically show smaller substrate conversion rates due to increased diffusional restrictions. The explanation for the unexpected increase in enzymatic activity of the larger 15 µm sized particles could be a higher internal surface area as compared to the smaller 6.5 µm templates. Indeed, the 15 µm templates exhibit a finer internal

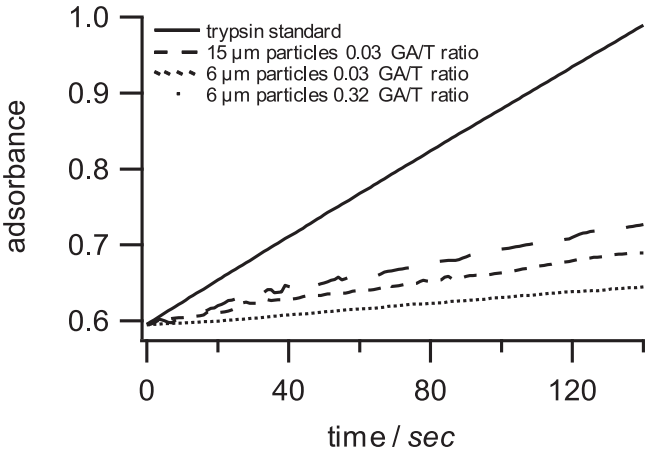

Figure 3. Activity of 6.5 and 15 µm trypsin particles for two different glutaraldehyde (GA) and trypsin (T) ratios.

structure with typical crystallites of 30 nm in size.[29] (Supporting Information, S5) whereas the 6.5 µm templates show larger crystallites with typical crystallite sizes of 30–100 nm (Supporting Information S4). As a result, the internal surface area and thus the activity of the larger trypsin particles is increased. Furthermore, the increase in activity for larger particles indicates the absence of substrate and reaction product diffusion limitations. This could be due to the high water content and pore size (≈60 nm) that is much larger than the size of substrate and product (below 1 nm). This shows that these particles could be used as catalysts also for high macromolecular weight substrates.

The activity measurement showed that the prepared trypsin particles might as well function as a CLEA for biotechnological processes. However, the key feature of the presented templating approach is that the individual particles have similar properties and thus a lower polydispersity as compared to standard CLEAs. Although this is not a major requirement in biotechnological catalysis, low polydispersity is a chief requirement for advanced applications, e.g. in biomedicine. In that respect, the porous protein particles might be interesting because of their well defined size and internal structure. As first basic example we considered porous hemoglobin particles as potential oxygen carrier and substitute for erythrocytes. To test the feasibility of this idea we determined the oxygen binding of the particles' heme groups by UV-vis spectroscopy (**Figure 4**).[24,33] First we analyzed oxygen free (deoxyhemoglobin) particles by adding the reducing agent sodium dithionite into our hemoglobin particles. Due to light scattering of the particles the hemoglobin spectra were altered, but as expected, the Soret band appears at a wavelength larger than 220 nm, typical for heme groups lacking associated oxygen. After removal of sodium dithionite by dialysis, hemoglobin oxidized again and bound oxygen as signified by the shift of the Soret band to a smaller wavelength (210 nm). Typical bands of oxyhemoglobin were also found between 542 nm and 577 nm (Figure 4 insets) after removal of the reducing agent showing that the hemoglobin retained its basic function when prepared by $CaCO_3$ templating and GA crosslinking. More advanced experiments with this material

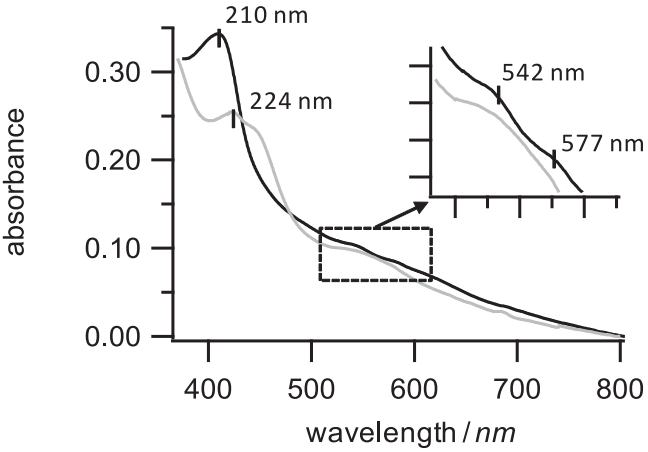

Figure 4. UV-vis spectra of deoxyhemoglobin (grey) and oxyhemoglobin particles (black).

should include oxygen dissociation measurements to obtain the oxygen transfer efficiency wich will be a focus of a separate future study. For clinical applications new strategies to suppress the potential leakage of harmful unbound or cleaved hemoglobin form the particles have to be developed as well.[24,25]

2.3. Hemoglobin Particles: Mechanical Properties

One of the important consequences of porous structures is a drastically decreased material stiffness as compared to non-porous structures. This was shown by AFM force-deformation measurements on porous and non-porous hemoglobin particles (**Figure 5**A). The AFM force measurements on non-porous hemoglobin were conducted by drying a solution of hemoglobin on a glass coverslip. The resulting hemoglobin film was then crosslinked using a GA/protein weight ratio of 0.03, the same procedure as for the porous particles. AFM nanoindentation in PBS buffer revealed elastic moduli on the order of 4 MPa, typical for non-crystalline, partially swollen protein aggregates.[34] The elastic moduli of porous hemoglobin particles were determined by AFM colloidal probe force measurements, a standard method to determine the mechanical properties of colloidal particles.[35,36] The obtained elastic moduli were 4.0 ± 1.41 kPa, three orders of magnitude smaller than for the non-porous hemoglobin film. Thus, the porous scaffold indeed leads to high material compliance when compared to non-porous systems and particles with unstable pores: In our previous studies on protein particles prepared by isoelectric precipitation[20] the particle elastic moduli was several hundred kPa, similar to the hemoglobin film, thus much larger as compared to the presented porous hemoglobin particles. Therefore the low elastic modulus of the porous particles further shows that by GA crosslinking the porous structure could be stabilized.

Next, we aimed at modulation of the elastic modulus by varying the degree of crosslinking. The GA/hemoglobin weight ratio was adjusted between 0.003 and 0.3 (Figure 5B). The molar ratio between the aldehyde groups of GA and primary amines of hemoglobin is varied between 0.07 and 7, accordingly. As expected, when reducing the crosslinker ratio the elastic modulus decreases. However, the modulus showed almost no changes when increasing the crosslinker ratio from 0.03 to 0.3. This could be explained by oversaturation of the crosslinkable primary amines at high concentration of glutaraldehyde. A crosslinker ratio below 0.003 resulted in non-stable protein particles. Moreover, the distribution of elastic moduli was rather broad (Figure 5 inset). This could be explained by a non homogeneous formation of pores during preparation of the $CaCO_3$ templates and variation of the protein content. On the other hand, the standard deviation of the elastic modulus did not exceed 35% implying a relatively uniform deformation behavior considering the complex internal structure of the particles. Moreover, in the applied force range of 12 nN, the particles exhibited almost no plastic (permanent) deformation (Supporting Information S7). This implies that the particles can completely recover their shape after mechanical deformation.

The high deformability of the porous hemoglobin particles may allow the particles to overcome obstacles in hydrodynamic flow, for example narrow blood vessels and in vivo filtration barriers like the liver or spleen.[37] To investigate the ability of the porous hemoglobin particles to deform in hydrodynamic flow, we conducted a simple microfluidic experiment. We designed microchannels that were 5-µm tall, 3 µm wide and several millimeters long (Figure 5). The channels were capped by a coverslip to avoid flow above the channels and to force traverse motion of the particles along the channels. The flow was generated by capillary forces drawing the particle dispersion into the channels. This can be done by simply placing the particle dispersion on a dry and hydrophilic microchannel

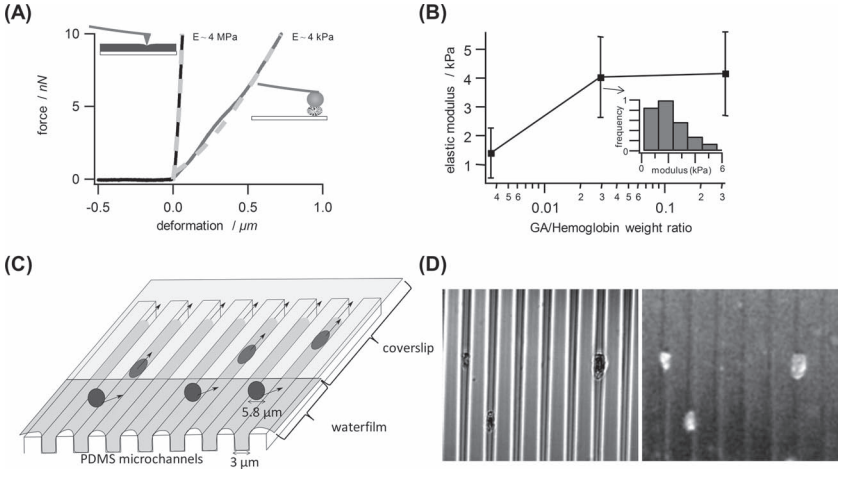

Figure 5. Mechanical characterization and deformability of hemoglobin. A) AFM colloidal probe force deformation measurements, typical force curves (solid lines in black and grey for, respectively, film and particle), and elastic modulus calculated via Hertz theory (dashed lines). B) Elastic moduli of hemoglobin particles as a function of the degree of crosslinking. C) Sketch of the deformation experiment in microchannels. D) Deformed hemoglobin particles in microchannels after flow; phase contrast (right) and autofluorescence (left).

structure near the rim of the coversplip. This procedure results in relatively large flow rates beneath the coversplip of about 1 mm/sec (1.5×10^{-8} mL/s along one channel). After the channel was filled with the dispersion, the particles were found stretched in the channel, increased in length by a factor of two (Figure 5D). This indicates that the particles can pass through channels that are smaller than the particle diameter. Also red blood cells (≈6 μm) must deform in such a way to traverse the sinusoids of the liver or spleen that are smaller than the cell. Therefore, when this ability is introduced on artificial systems like drug carriers or red blood cell mimicries, their circulation time in the vascular system can be significantly increased.[37] From the elastic behavior as determined by AFM experiments (Figure 5A), we can also assume that the particles would relax from the deformed state when they enter wider channels, similar to natural red blood cells.[38] Overall, the porous structure of protein particles ensures high deformability upon flow making them potentially useful for biomedical applications targeting the vascular system.

3. Conclusions

Taken together, infiltration of porous colloidal $CaCO_3$ templates by drying of a protein solution followed by GA crosslinking and dissolution of the templates by EDTA allows for the preparation of porous protein particles. The method is extremely versatile in that virtually any protein can be transformed into particulate form by this approach. Furthermore the size of the particles can be conveniently controlled by the template. Analysis by optical microscopy, cryo-SEM, AFM and dextran diffusion revealed that the particles possess a well controlled morphology suggesting that the porous structure of the $CaCO_3$ templates was successfully replicated. Moreover, we could show that the protein particles remained functional after templating. As an example we studied the activity of trypsin particles and found activities on the order of 25% as compared to non-crosslinked trypsin. The surface area of the particles can be expected to be comparable to that of the calcium carbonate templates (8 m^2/g).[22] This would be very useful, for example in catalysis when particles composed of enzymes are formed. In regard to industrial biocatalytic applications of the enzyme particles the long term stability as well as their repeated usage will be tested. Comparison of the elastic properties of porous particles and non-porous films made from hemoglobin indicates that the porous systems posses a low density and that the pores are stable against collapse. As a result the elastic modulus was drastically decreased for the porous particles and the particle deformation was reversible, almost completely elastic. By varying the degree of crosslinking particles with a modulus in the kPa range can be fabricated, similar to the stiffness of red blood cells, thus potentially allowing for long circulation time in the vascular system. Besides general applications as drug carrier the hemoglobin particles presented in this work may have potential as artificial red blood cell because of their suitable size and mechanical properties as well as the ability to take up oxygen. Also the high internal surface area could enhance the oxygen carrying capacity.

In future studies we will therefore further investigate oxygen binding under different partial pressures to evaluate if the of porous hemoglobin particles could act as artificial blood cells. Preparation of sub-micrometer sized protein particles by using smaller template particles[39] may also enable new biomedical applications. In this regard, the cellular uptake of such smaller and soft (deformable) particles will be a focus of our future study to understand fundamental aspects of intercellular forces and applications for intracellular delivery.

4. Experimental Section

Materials: All chemicals were purchased from Sigma-Aldrich (Germany). Hemoglobin, lysozyme, trypsin and FITC dextran- (500 kDa and 2000KDa) were obtained as lyophilized powder. Aliquots of GA (grade I, 25% in water) were stored at −20 °C. Sodium sulfate, and buffers where obtained as dry powder, p.a. and bioreagent grade, respectively. The calcium carbonate templates (average diameter 6.5 and 15.2 μm) were synthesized as described elsewhere.[20,22]

Preparation of Porous Protein Particles: First a protein/$CaCO_3$ template dispersion (0.5 mL, 50 mg of $CaCO_3$) was prepared in purified water. The protein/$CaCO_3$ weight ratio was kept constant at 7%. Then the water was removed on a rotary evaporator (150 mbar, 25 °C). After about two hours the water is completely evaporated and the templates were redispersed in 4 M Na_2SO_4 (pH 9, 20 mM carbonate buffer). Vigerous agitation and application of ultrasound (Elmasonic P30 H, 130 W) for two minutes then yields redispersed protein-filled $CaCO_3$ templates. The particles were then crosslinked via GA at a concentration of 0.00025-–.025 M which translates to 0.003-0.3 w/w with respect to the protein. After three-fold centrifugation and washing the $CaCO_3$ templates were dissolved in 0.2 M EDTA (pH 8, NaOH adjusted). Finally, residual EDTA, the complex Ca-EDTA and bicarbonate were removed by dialysis in PBS using Float-A-Lyzers G2 with a size cutoff of 50 kD (Spectrum Laboratories Inc, USA).

Microscopy: Optical microscopy was conducted on an Olympus IX 51 equipped with a Zeiss HRm camera. Phase contrast and fluorescence images were collected with a 20× Objective (PLN 20XPH, N.A. 0.4, Olympus, Japan). High resolution optical images were taken in brightfield with a 63× Objective (Antiflex Neofluar, N.A. 1.45, Zeiss, Germany). The porosity of $CaCO_3$ templates and protein particles was investigated utilizing a scanning electron microscope (SEM) LEO 1550 operating at 3 kV, a scanning electron microscope JEOL JSM-7500F operating at 2 kV for cryogenic study (cryo-SEM) and a transmission electron microscope (TEM) Zeiss EM 912 Omega operating at 120 kV. AFM imaging of dried protein particles was conducted with a Nanowizard I (JPK instruments AG, Germany) in tapping mode using a standard silicon cantilever with a nominal spring constant of 40 N/m (NSC16, MicroMash, Estonia).

Permeability Studies: The porosity of the protein particles was tested in a permeability study using FITC-labeled dextran of different molecular weight 500 kDa and 2000 kDa. The dextrans were added to the protein particles suspension to obtain a dextran concentration about 1 μg/mL. Then CLSM micrographs were taken with a Leica confocal scanning system mounted on a Leica Aristoplan apparatus and quipped with a 100× oil immersion objective (numerical aperture 1.4) From the images the fluorescence intensity within more than 20 particles was determined using image processing (ImageJ 1.4, NHS, USA). The data was normalized using the background fluorescence intensity. In the time frame of the image acquisition (2 h) and after incubation over night no changes in the particles fluorescence were observed.

Micromechanical Characterization: The elastic properties of the protein particles were measured via colloidal probe AFM. As force probe we used colloidal silica particles (Microparticles GmbH, Berlin, Germany) with a diameter of 30 μm glued to the apex of the AFM cantilevers with a spring constant of 0.03 N/m (CSC12, tipless, MicroMash, Estonia). Prior to the probe attachment the spring constant was determined according to the thermal noise[40] and the Sader[41] method. The cantilevers showed deviation between both methods of less than 10% to qualify for force measurements. The protein particles were allowed

to sediment and adhere onto a polyethyleneimine coated coverslip[35] by which they are immobilized. The AFM head is mounted on an optical microscope (IX51, Olympus, Japan). Using bright field optics and also using the autofluorescence of the protein particles the colloidal probe was positioned at the apex of the microgels in order to perform the AFM force measurement. The measurement was conducted using an approach speed of 1 µm/s applying peak forces of 12 nN. The deformation of the particles upon hydrodynamic flow in microchannels involved preparation of a polydimethylsiloxane (PDMS, Sylgard 184, Dow Corning Germany) stamp from a lithographic silicon master with 3 µm grating (GeSim mbH, Germany) as described in.[42] The PDMS channels were covered with a glass coverslip. Capillary action drew the micrometer-sized protein particles into the channels (see Figure 5C) after placing a droplet of the particle dispersion near the rim of the coverslip. The deformed particles in the channels were then imaged by optical microscopy.

Enzymatic Activity of Trypsin Particles: The activity of porous trypsin particles was determined at 25 °C in 50 mM phosphate buffer, pH 7.4 using N-benzoyl-l-arginine ethyl ester (BAEE) as a substrate.[32] At BAEE excess concentration the conversion rate was compared to trypsin standard solutions to obtain a relative activity. The concentration of the trypsin in solution and in particulate form was 0.625 µg/mL during the photometric assay. Residual enzymatic activity in the supernatant of centrifuged particle dispersion was less than 1% compared to the particle suspension. The measurements were conducted on a JASCO V 400 spectrophotometer at 514 nm.

Supporting Information

Supporting Information is available from the Wiley Online Library or from the author.

Acknowledgements

D.V. thanks the Alexander von Humboldt Foundation for support (AvH Fellowship and Sofja Kovalevskaja Program). The authors thank Dr. Jürgen Hartmann for SEM and TEM imaging.

Received: May 15, 2012
Revised: June 29, 2012
Published online: August 13, 2012

[1] S. X. Yang, W. E. Yuan, T. Jin, *Expert Opin. Drug Delivery* **2009**, *6*, 1123.
[2] D. V. Volodkin, R. von Klitzing, H. Möhwald, *Angew. Chem. Int. Ed.* **2010**, *49*, 9258.
[3] a) S. K. Basu, C. P. Govardhan, C. W. Jung, A. L. Margolin, *Expert Opin. Biol. Ther.* **2004**, *4*, 301; b) S. Pechenov, B. Shenoy, M. X. Yang, S. K. Basu, A. L. Margolin, *J. Controlled Release* **2004**, *96*, 149.
[4] a) W. Wang, *Int. J. Pharm.* **2000**, *203*, 1; Y. F. Maa, P. A. Nguyen, T. Sweeney, S. J. Shire, C. C. Hsu, *Pharm. Res.* **1999**, *16*, 249; b) S. Stolnik, L. Illum, S. S. Davis, *Adv. Drug Delivery Rev.* **1995**, *16*, 195; c) M. L. Tan, P. F. M. Choong, C. R. Dass, *Peptides* **2010**, *31*, 184; d) F. Caruso, H. Mohwald, *J. Am. Chem. Soc.* **1999**, *121*, 6039.
[5] a) D. V. Volodkin, N. G. Balabushevitch, G. B. Sukhorukov, N. I. Larionova, *STP Pharm. Sci.* **2003**, *13*, 163; b) D. V. Volodkin, N. G. Balabushevitch, G. B. Sukhorukov, N. I. Larionova, *Biochem.-Moscow* **2003**, *68*, 236.
[6] R. A. Sheldon, *Appl. Microbiol. Biotechnol.* **2011**, *92*, 467.
[7] U. Roessl, J. Nahalka, B. Nidetzky, *Biotechnol. Lett.* **2010**, *32*, 341.
[8] a) L. Q. Cao, F. van Rantwijk, R. A. Sheldon, *Org. Lett.* **2000**, *2*, 1361; b) P. Lopez-Serrano, L. Cao, F. van Rantwijk, R. A. Sheldon, *Biotechnol. Lett.* **2002**, *24*, 1379.
[9] H. W. Yu, H. Chen, X. Wang, Y. Y. Yang, C. B. Ching, *J. Mol. Catal. B-Enzym.* **2006**, *43*, 124.
[10] N. A. Pchelintsev, M. I. Youshko, V. K. Svedas, *J. Mol. Catal. B-Enzym.* **2009**, *56*, 202.
[11] R. Schoevaart, M. W. Wolbers, M. Golubovic, M. Ottens, A. P. G. Kieboom, F. van Rantwijk, L. A. M. van der Wielen, R. A. Sheldon, *Biotechnol. Bioeng.* **2004**, *87*, 754.
[12] a) J. A. Champion, A. Walker, S. Mitragotri, *Pharm. Res.* **2008**, *25*, 1815; b) Y. Geng, P. Dalhaimer, S. S. Cai, R. Tsai, M. Tewari, T. Minko, D. E. Discher, *Nat. Nanotechnol.* **2007**, *2*, 249; c) P. Decuzzi, R. Pasqualini, W. Arap, M. Ferrari, *Pharm. Res.* **2009**, *26*, 235; d) K. A. Beningo, Y. L. Wang, *J. Cell Sci.* **2002**, *115*, 849.
[13] a) P. Schmidt-Winkel, W. W. Lukens, P. D. Yang, D. I. Margolese, J. S. Lettow, J. Y. Ying, G. D. Stucky, *Chem. Mater.* **2000**, *12*, 686; b) P. Zhang, Z. Weng, J. Guo, C. Wang, *Chem. Mater.* **2011**.
[14] P. Innocenzi, L. Malfatti, T. Kldchob, P. Falcaro, *Chem. Mater.* **2009**, *21*, 2555.
[15] a) H. W. Yan, C. F. Blanford, B. T. Holland, W. H. Smyrl, A. Stein, *Chem. Mater.* **2000**, *12*, 1134; b) N. Ritter, I. Senkovska, S. Kaskel, J. Weber, *Macromolecules* **2011**, *44*, 2025.
[16] R. Vogel, M. Persson, C. Feng, S. J. Parkin, T. A. Nieminen, B. Wood, N. R. Heckenberg, H. Rubinsztein-Dunlop, *Langmuir* **2009**, *25*, 11672.
[17] a) A. Thomas, F. Goettmann, M. Antonietti, *Chem. Mater.* **2008**, *20*, 738; b) X. S. Zhao, F. B. Su, Q. F. Yan, W. P. Guo, X. Y. Bao, L. Lv, Z. C. Zhou, *J. Mater. Chem.* **2006**, *16*, 637; c) A. Thomas, P. Kuhn, J. Weber, M. M. Titirici, M. Antonietti, *Macromol. Rapid Commun.* **2009**, *30*, 221.
[18] Q. Li, M. Retsch, J. Wang, W. Knoll, U. Jonas, in *Templates in Chemistry Iii*, Vol. *287*, (Ed: P. Broekmann, C. Schalley), Springer, Berlin/Heidelberg **2009**, p. 135.
[19] a) Y. J. Wang, F. Caruso, *Adv. Mater.* **2006**, *18*, 795; b) Y. Wang, A. Yu, F. Caruso, *Angew. Chem. Int. Ed.* **2005**, *44*, 2888.
[20] D. Volodkin, S. Schmidt, P. Fernandes, G. Sukhorukov, L. NI, H. Möhwald, R. von Klitzing, *Adv. Funct. Mater.* **2012**, *22*, 1914.
[21] a) D. V. Volodkin, N. I. Larionova, G. B. Sukhorukov, *Biomacromolecules* **2004**, *5*, 1962; b) G. B. Sukhorukov, D. V. Volodkin, A. M. Günther, A. I. Petrov, D. B. Shenoy, H. Möhwald, *J. Mater. Chem.* **2004**, *14*, 2073; c) H. Baumler, R. Georgieva, *Biomacromolecules* **2010**, *11*, 1480.
[22] D. V. Volodkin, A. I. Petrov, M. Prevot, G. B. Sukhorukov, *Langmuir* **2004**, *20*, 3398.
[23] a) J. Zhao, C. S. Liu, Y. Yuan, X. Y. Tao, X. Q. Shan, Y. Sheng, F. Wu, *Biomaterials* **2007**, *28*, 1414; b) W. Gao, B. Y. Sha, W. Zou, X. Liang, X. Z. Meng, H. Xu, J. Tang, D. C. Wu, L. X. Xu, H. Zhang, *Biomaterials* **2011**, *32*, 9425; c) Y. Sheng, C. S. Liu, Y. Yuan, X. L. Zhang, X. Q. Shan, F. Xu, *J. Biomed. Mater. Res. Part B* **2009**, *91B*, 631.
[24] T. H. Li, X. B. Jing, Y. B. Huang, *Macromol. Biosci.* **2011**, *11*, 865.
[25] a) T. M. S. Chang, *J. Intern. Med.* **2003**, *253*, 527; b) F. A. Moore, B. A. McKinley, E. E. Moore, *Lancet* **2004**, *363*, 1988.
[26] M. F. Wang, W. Qi, R. X. Su, Z. M. He, *Prog. Chem.* **2010**, *22*, 173.
[27] L. Brecevic, D. Kralj, *Croat. Chem. Acta* **2007**, *80*, 467.
[28] O. Kreft, R. Georgieva, H. Baumler, M. Steup, B. Muller-Rober, G. B. Sukhorukov, H. Mohwald, *Macromol. Rapid Commun.* **2006**, *27*, 435.
[29] M. Behra, S. Schmidt, J. Hartmann, D. V. Volodkin, L. Hartmann, *Macromol. Rapid Commun.* **2012**, *33*, 1049.
[30] a) E. C. Valdes, L. W. Soto, G. A. Arcaya, Electron. *J. Biotechnol.* **2011**, 14; b) P. Gupta, K. Dutt, S. Misra, S. Raghuwanshi, R. K. Saxena, *Bioresour. Technol.* **2009**, *100*, 4074.
[31] J. K. Armstrong, R. B. Wenby, H. J. Meiselman, T. C. Fisher, *Biophys. J.* **2004**, *87*, 4259.
[32] G. W. Schwert, Y. Takenaka, *Biochim. Biophys. Acta* **1955**, *16*, 570.
[33] S. F. Hou, J. H. Wang, C. R. Martin, *Nano Lett.* **2005**, *5*, 231.
[34] S. Guo, B. B. Akhremitchev, *Langmuir* **2008**, *24*, 880.

[35] S. Schmidt, P. A. L. Fernandes, B. G. De Geest, M. Delcea, A. G. Skirtach, H. Mohwald, A. Fery, *Adv. Funct. Mater.* **2011**, *21*, 1411.
[36] a) P. A. L. Fernandes, S. Schmidt, M. Zeiser, A. Fery, T. Hellweg, *Soft Matter* **2010**, *6*, 3455; b) A. Fery, R. Weinkamer, *Polymer* **2007**, *48*, 7221.
[37] T. J. Merkel, S. W. Jones, K. P. Herlihy, F. R. Kersey, A. R. Shields, M. Napier, J. C. Luft, H. L. Wu, W. C. Zamboni, A. Z. Wang, J. E. Bear, J. M. DeSimone, *Proc. Natl. Acad. Sci. USA* **2011**, *108*, 586.
[38] J. L. McWhirter, H. Noguchi, G. Gompper, *Proc. Natl. Acad. Sci. USA* **2009**, *106*, 6039.
[39] W. Wei, G.-H. Ma, G. Hu, D. Yu, T. McLeish, Z.-G. Su, Z.-Y. Shen, *J. Am. Chem. Soc.* **2008**, *130*, 15808.
[40] J. L. Hutter, J. Bechhoefer, *Rev. Sci. Instrum.* **1993**, *64*, 1868.
[41] J. E. Sader, *J. Appl. Phys.* **1998**, *84*, 64.
[42] S. Schmidt, M. Nolte, A. Fery, *Phys. Chem. Chem. Phys.* **2007**, *9*, 4967.